Diagnostics in Disassembly Unscrewing Operations

DANIEL W. APLEY
Department of Mechanical Engineering and Applied Mechanics, University of Michigan, Ann Arbor

GÜNTHER SELIGER AND LORENZ VOIT
Institute for Machine Tools and Manufacturing Technology, Technical University Berlin, Germany

JIANJUN SHI
Department of Industrial and Operations Engineering, University of Michigan, Ann Arbor

Abstract. Disassembly for recycling purposes is an emerging area of research that offers many advantages over more traditional means of recycling. However, many technical challenges are involved in automated disassembly. This paper addresses one of the critical challenges involved: diagnostics in the unscrewing operation. The various conditions that can arise when one attempts to unscrew a screw (one of which is the successful removal of the screw) are categorized, and a diagnostic procedure for detecting which condition has occurred and deciding what subsequent action to take is developed. Experimental condition detection results are presented.

Key Words: disassembly, recycling, diagnostics, least squares

1. Introduction

The recycling of technical consumer products is a subject in which interest is rapidly increasing, due to the growing importance of conserving energy, material resources, and landfill capacity. Many governments worldwide are stiffening legislation requiring manufacturers to play a role in recycling products at their end of life. This is especially true in areas of high population density, such as Germany and Japan, where resources and landfill capacity are limited (Seliger and Hentschel, 1994; Seliger, Hentschel, and Kriwet, 1993). The landfill disposal cost in Germany exploded from 20 DM/ton in 1987 to 1000 DM/ton in 1993 (Seliger et al., 1993). In special purpose landfills, where products containing hazardous substances must be disposed, the cost was over 3000 DM/ton by 1993.

Of all the recycling options, disassembly, or partial disassembly, is one of the most promising. Disassembly makes possible the reuse of entire subcomponents, more effective isolation of pure materials for reutilization, and isolation of hazardous substances, minimizing the waste that must be disposed of in special purpose landfills. Overviews and examples of disassembly process planning can be found in Seliger and Hentschel (1994) and Seliger et al. (1993).

Much of the disassembly research to date deals with designing the product with disassembly in mind. Such design for disassembly is considered in Navin-Chandra (1991), Zussman, Kriwet, and Seliger (1994), and Boothroyd and Alting (1992). Another area of research concerns how to determine the optimum recycling strategy, in terms of the order in which

to disassemble a product and how far to disassemble it. Hentschel, Seliger, and Zussman (1994, 1995) present reactive approaches for doing this, which evaluate the recyclability of an incoming product and update the disassembly strategy based on this information.

Currently, most disassembly facilities are based on manual operations with limited automated machinery (de Ron and Penev, 1995; Langerak, 1997; Kopacek and Kronreif, 1996). However, manual disassembly operations are not well suited to deal with the recycling scenario of the near future. The tremendous quantities of technical consumer products that will need to be recycled necessitates automation, or at least partial automation, of the disassembly process (Kopacek and Kronreif, 1996; Feldmann and Scheller, 1994). In addition, manual disassembly often is monotonous, unpleasant, or even hazardous work (Weigl, 1994; de Ron and Penev, 1995), an extreme case being the disassembly of explosive devices (Ray, 1996). Consequently, considerable attention has been given recently to designing automated disassembly operations. Most of the products for which automated disassembly has been investigated fall into the category of consumer electronics; examples include keyboards (Langerak, 1997), personal computers (Kopacek and Kronreif, 1996), televisions (Jorgensen, Andersen, and Christensen, 1996), and printed circuit boards (Feldmann and Scheller, 1994). The large scale on which these types of products are manufactured and discarded generally is the strongest motivating factor for automating their disassembly process.

A key issue in the automated disassembly of a product is the type of fasteners used to assemble the product. The most common fasteners are threaded (Phillips and slot head screws and hex head bolts); rivets; snap joints; welded, brazed, and soldered joints; and adhesives (Juvinal, 1983). Of these, only threaded fasteners can be removed in a nondestructive manner. Removal of nonthreaded fasteners requires cutting the components or fastener. Since this would be highly application specific, developing generic strategies for removing nonthreaded fasteners would be more difficult. Consequently, this paper focuses on nondestructive disassembly and assumes that the product components to be disassembled are fastened by screws or bolts (unless otherwise indicated, subsequently referred to as simply *screws*).

Suppose that the product is located on a fixture and ready to be disassembled. The following three tasks must be successfully accomplished: (1) The screws must be located; (2) after locating the screws, they must be removed; and (3) after removing the screws, the components must be separated. A prototype vision system for locating screws has been developed by the second author, with successful tests conducted in a laboratory environment. Other research on vision systems in automated disassembly can be found in Jorgensen et al. (1996), Feldmann and Scheller, (1994), Weigl, (1994), and Dario, Rucci, Guadagnini and Laschi, (1994). In the future, the success of such vision systems may be greatly improved by providing manufacturers' specifications giving descriptions and nominal locations of all screws. The third task is considered, for example, in Dutta and Woo (1995) and relies heavily on design for disassembly.

This paper focuses on the second task, for which it is assumed that a screwdriver (or a wrench for hex head bolts) held by a robotic manipulator is the tool used to remove the screws. After locating a screw, attempting to engage the head of the screw with the screwdriver, and attempting to remove the screw, the actual state of the system must be correctly diagnosed. Specifically, is the screw coming out and, if not, why not?

The remainder of the paper is as follows. The various conditions that are likely to arise in the unscrewing process are categorized and modeled in Sections 2 and 3. In Section 4, a diagnostic algorithm is developed for detecting which condition has occurred, and a scheme for taking subsequent action is presented. Section 5 provides experimental results illustrating the effectiveness of the diagnostic algorithm.

2. Categorizing the unscrewing conditions

This section explains and categorizes the various conditions that could arise and need to be detected during the unscrewing process. The categorization is both qualitative and quantitative, in terms of the appropriate process signals being measured.

One of the results of this research is that measurement of the unscrewing torque and shaft rotation provides reliable signals with rich enough information to distinguish among the different conditions that arise. Equally important, these signals can be measured very economically, with little extra hardware required.

The experimental setup used in this research is shown in figure 1. A screwdriver powered by a 7.5 volt dc motor is attached to a vertical shaft, on which it can be moved up and down or locked into place. A potentiometer is used to measure the angle of rotation of the shaft (θ), and a shunt is used to measure the current through the motor. The time constant of the motor circuitry is fast enough, relative to the frequency content of the torque signal, that it can be assumed the measured current is proportional to the motor torque (T). Both signals are sent to a data acquisition (DAQ) board in a PC, where the signal analysis takes place. The DAQ hardware consists primarily of analog to digital converters for sampling the torque and shaft rotation signals, anti-aliasing filters, and a couple of digital to analog output channels for controlling the experiment.
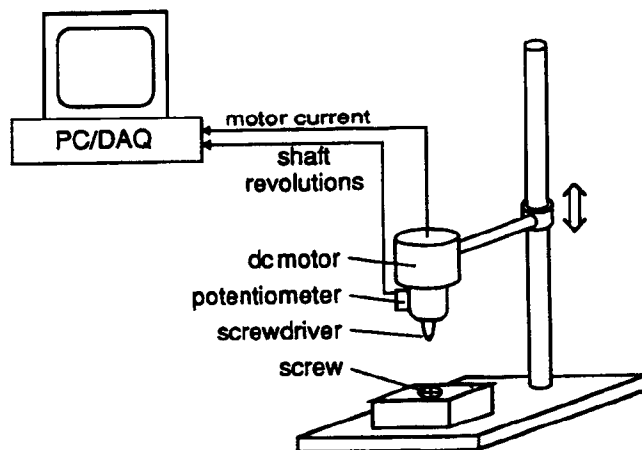

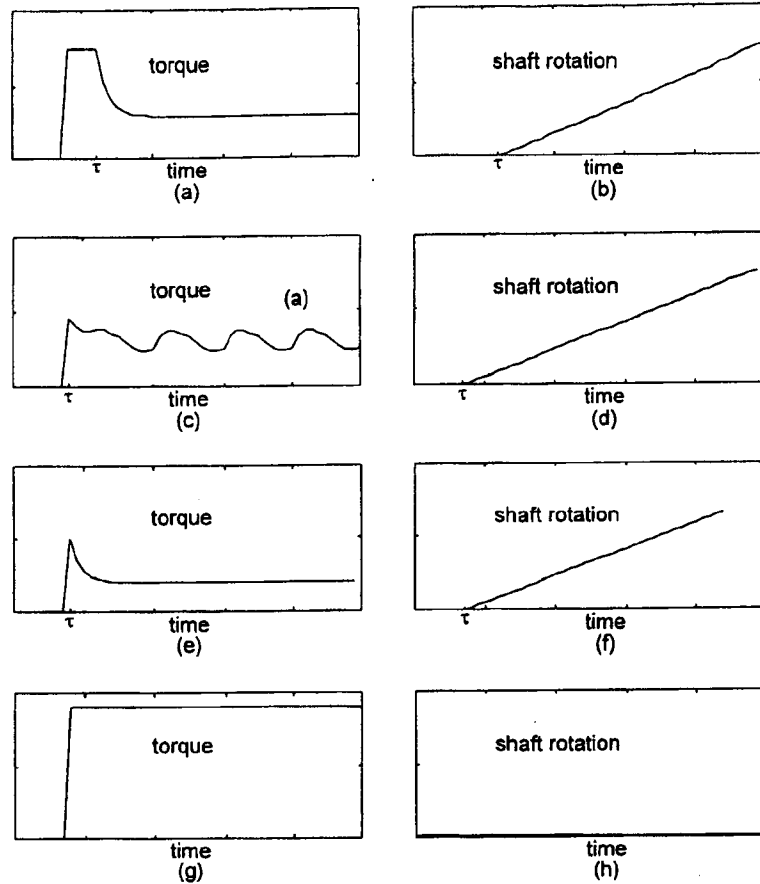
Figure 1. Experimental setup.

Figure 2. Behavior of the measured signals under each unscrewing condition. (a) and (b) screw coming out; (c) and (d) screwdriver slipping on head of screw; (e) and (f) screwdriver missed screw; (g) and (h) screw too tight to move.

The four most commonly occurring conditions that may arise in the unscrewing process are explained in the following paragraphs, and their effects on the measured signals are shown in figure 2. The signals illustrated in figure 2 are not meant to be quantitatively precise but rather only an approximate qualitative representation to provide an idea of how the T and θ signals differ under each condition. The conditions are numbered 0 to 3, as follows.

Condition 0 (screw coming out): The screwdriver properly engages the head of the screw and, when a voltage is applied, the screw comes out. T (figure 2(a)) reaches some peak torque, where it remains (approximately) constant while the screw breaks free. At time τ the screw begins moving, at which time θ (figure 2(b)) begins to increase monotonically and T decays to some steady-state value required to keep the screw turning.

Condition 1 (screwdriver slipping on the head of the screw): As in condition 0, the screwdriver properly engages the head of the screw. However, when a voltage is applied, the screwdriver slips on the head of the screw. This situation occurs commonly when unscrewing Phillips head screws that are old and rusted or made of soft, low-quality metal. The direct cause is the edges of the slots on the head of the screw becoming rounded. In the case of a hex head bolt, it could result from the corners of the bolt head becoming rounded. T (figure 2(c)) reaches some peak value, at which time the screwdriver starts to slip, and θ (figure 2(d)) begins to increase monotonically. As the screwdriver slips on the head of the screw, a periodic torque signal is produced. The frequency of this periodic signal would be four times the shaft rpm (for a Phillips head screw) or six times the shaft rpm (for a hex head bolt). The experimental data presented later in this paper demonstrate that this assumed torque profile is a quite reasonable approximation of the actual torque signal.

Condition 2 (screwdriver missed the head of the screw): Condition 2 assumes the head of the screw was missed when the screwdriver was moved to engage it, due to an error in locating the screw or inaccuracies in the robotic arm supporting the screwdriver. As a result, when a voltage is applied, the shaft begins rotating immediately "on air" or on a flat surface and θ (figure 2(f)) increases monotonically. Some peak torque is reached while the mass of the screwdriver is accelerated, after which time, T (figure 2(e)) decays to a (possibly low) steady-state value.

Condition 3 (screw too tight to move): The screwdriver properly engages the head of the screw, but when a voltage is applied the torque is not sufficient to free the screw. In this case, T (figure 2(g)) reaches some peak value, where it remains constant and θ (figure 2(h)) remains 0.

Detecting condition 3 is trivial, since it is the only one of the four conditions under which θ does not change. Consider conditions 0 and 2, which clearly cannot be distinguished on the basis of θ (θ could be identical for each of conditions 0–2). Neither does T provide a reliable means of distinguishing between conditions 0 and 2, since the magnitude of the peak and steady-state torque and the duration of the peak torque depend on many factors. However, detecting whether condition 2 has occurred can be achieved as follows. After the screwdriver is moved into position to engage the screw but before applying a counterclockwise torque to remove the screw, apply a small clockwise torque that is large enough to overcome friction and rotate the screwdriver but not so large as to overtighten the screw. If the screwdriver rotates freely in the clockwise direction (which can be easily determined from θ) then it can be concluded that condition 2 has occurred. On the other hand, if the screwdriver does not rotate in the clockwise direction, then it can be concluded that one of conditions 0, 1, or 3 will occur. In this event, after subsequently attempting to remove the screw with a counterclockwise torque, condition 3 can be effectively detected or eliminated as previously discussed.

To summarize the main points of this section, conditions 2 and 3 can be easily detected, reducing the problem to that of detecting either condition 0 or condition 1. Consequently, much of the remainder of the paper focuses on that problem.

Condition 1, although common for hex head bolts and Phillips head screws, would be less likely to occur for slot head screws. Instead of the screwdriver remaining centered and

slipping on the head of the screw, it would be more likely that the screwdriver would pop out of the head of the screw. The algorithm developed in Sections 3 and 4 is designed to distinguish conditions 0 and 1 and therefore, would, not be applicable to slot head screws. However, problems with slot head screws still are partially diagnosable, since the procedure for distinguishing conditions 2 and 3 would apply.

It should be noted that an alternative to unscrewing the screws is to cut them out; for example, via milling or drilling. However, this is less desirable than removing them nondestructively, which would allow greater reusability of the components of the product—one of the goals of disassembly. In addition, cutting the screw could leave burrs that cause interference when attempting to disassemble the components. This would likely require more human interaction than if the screws were unscrewed. Consequently, the focus of this paper is on removing the screws nondestructively.

3. Modeling the torque signal

Figure 3 shows the two torque profiles corresponding to conditions 0 and 1 for two complete shaft revolutions for a Phillips head screw. A pronounced periodic component of frequency four times the shaft rotational frequency is evident in the torque profile for condition 1. Since this component is much less dominant under condition 0, this will serve as the basis for distinguishing between the two conditions.

The signals shown in figure 3 are in units of volts, rather than torque, and are voltage drops across the shunt. The signal has been filtered to remove high-frequency components. In addition, the signal has been resampled (using interpolation) so that the sampling is uniform with respect to shaft rotation, which is crucial in the subsequent analysis. The reason is that the original torque signal is sampled uniformly with respect to time. If the rotational
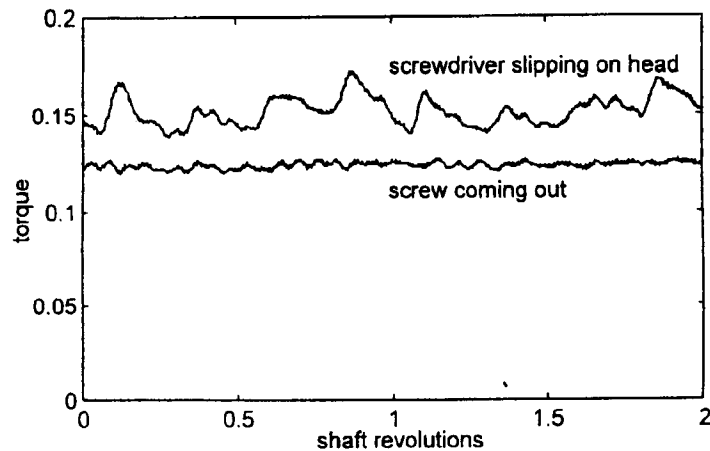

Figure 3. Resampled torque profiles for two shaft revolutions for a Phillips head screw.

frequency of the shaft were not constant, then the frequency of the periodic component also would vary. In contrast, if the torque signal were sampled uniformly with respect to shaft rotation, the frequency of the periodic component (in radians/sample) would be known and constant.

Let ω denote the shaft rotational frequency in radians/sample. Under either condition the torque signal is approximately periodic with fundamental frequency ω. By Fourier's theorem it can be represented as a summation of sinusoids with frequencies $\{0, \omega, 2\omega, 3\omega, \ldots\}$. In practice, the signal can be approximated by a finite number of these sinusoids. Condition 0 represents the screw coming out of the hole. If the screw has a burr on the shaft, this could result in a significant ω frequency component. If the screw and hole are slightly ellipsoidal, this could cause binding every half revolution of the screw and result in a significant 2ω frequency component. Higher harmonics also may be present, but their magnitude is not likely to be as large. Under condition 1 also, the signal may be approximated by a finite number of sinusoids of frequency $\{0, \omega, 2\omega, 3\omega, \ldots\}$. However, the signal will likely be dominated by a 4ω periodic component (for a Phillips head screw) that has harmonics of $4\omega, 8\omega, 12\omega, \ldots$ For the case of hex head bolts, the signal will be dominated by a 6ω periodic component that has harmonics of $6\omega, 12\omega, 18\omega, \ldots$ As evident in figure 3, the 4ω periodic component and its higher harmonics are far more significant under condition 1 than under condition 0. The presence of these frequency components will allow distinction between conditions 0 and 1.

In general, define Ω_1 to be the collection of all frequencies that may be significant under either condition 0 or 1. Let p_1 denote the number of frequencies in this set, excluding the 0 frequency, and enumerate Ω_1 as $\Omega_1 = \{0, \Omega_{1,i} : i = 1, 2, \ldots, p_1\}$. Define Ω to be the set of frequencies that are expected to be much more significant under condition 1 than under condition 0. Let p denote the number of frequencies in this set, and enumerate Ω as $\Omega = \{\Omega_i : i = 1, 2, \ldots, p\}$. Define Ω_0 to be the set difference $\Omega_1 - \Omega$; that is, the set of all frequencies in Ω_1 that are not in Ω. Finally, let p_0 denote the number of frequencies in this set, excluding the 0 frequency, and enumerate Ω_0 as $\Omega_0 = \{0, \Omega_{0,i} : i = 1, 2, \ldots, p_0\}$. Note that $\Omega_1 = \Omega_0 \cup \Omega$ and that $\Omega_1 \subset \{0, \omega, 2\omega, 3\omega, 4\omega, \ldots\}$.

Ω_1 must include all frequencies that may have significant energy under either condition, and Ω must include at least one frequency that is expected to have significantly more energy under condition 1 than under condition 0. Other than this, exactly what frequencies to include in these sets is somewhat arbitrary. Through intuition and experiments, it was found that $\Omega_1 = \{0, \omega, 2\omega, 3\omega, 4\omega, 8\omega, 12\omega, 16\omega, 20\omega\}$ and $\Omega = \{4\omega, 8\omega, 12\omega, 16\omega, 20\omega\}$ provided good results for Phillips head screws. Likewise, for hex head bolts $\Omega_1 = \{0, \omega, 2\omega, 3\omega, 4\omega, 5\omega, 6\omega, 12\omega, 18\omega, 24\omega, 36\omega\}$ and $\Omega = \{6\omega, 12\omega, 18\omega, 24\omega, 30\omega\}$ provided good results. The interpretation is that the $4\omega (6\omega)$ component and its higher harmonics are likely to have much more energy under condition 1 than under condition 0, due to the screwdriver (wrench) slipping on the head of the screw (bolt). Under either condition, very little signal energy was found resulting from components with frequency greater than 30ω, due in part to prefiltering the signal to avoid aliasing.

Suppose that, after resampling the torque signal uniformly in θ, one has N torque measurements, which are represented as an N-length column vector T. From the preceding paragraphs, T can be approximately represented as a linear combination of sampled sinusoids with frequencies in Ω_1. The difference between the measured T and the sinusoidal

approximation is assumed to be due to white Gaussian noise, which gives rise to the following mathematical model for T.

$$T = \begin{bmatrix} S_0 & S \end{bmatrix} \begin{bmatrix} \alpha_0 \\ \alpha \end{bmatrix} + W$$

W is an N-length random vector of white Gaussian noise with zero-mean and variance σ^2, denoted $W \sim N(0, \sigma^2 I)$. Here, 0 is a vector of zeros representing the mean vector of W, I is the $N \times N$ identity matrix, and $\sigma^2 I$ is the covariance matrix of W. S_0 and S are $N \times (2p_0 + 1)$ and $N \times 2p$ matrices with columns consisting of sampled sine or cosine functions with frequencies in Ω_0 and Ω, respectively. If $s_{0,i,j}$ and $s_{i,j}$ denote the ith row, jth column element of S_0 and S, respectively, then

$$\left. \begin{array}{l} s_{0,i,1} = 1 \\ s_{0,i,2j} = \sin(i\Omega_{0,j}) \\ s_{0,i,2j+1} = \cos(i\Omega_{0,j}) \end{array} \right\} \quad i = 1, 2, \ldots, N; \, j = 1, 2, \ldots, p_0 \tag{1}$$

$$\left. \begin{array}{l} s_{i,2j-1} = \sin(i\Omega_j) \\ s_{i,2j} = \cos(i\Omega_j) \end{array} \right\} \quad i = 1, 2, \ldots, N; \, j = 1, 2, \ldots, p \tag{2}$$

Here, α_0 is a $(2p_0 + 1)$-length vector containing the weighting coefficients for each of the sinusoids with frequency in Ω_0; and it determines the extent to which each of these sinusoids is present in the torque signal. Likewise, α is a $2p$-length vector that determines the extent to which the sinusoids with frequencies in Ω are present in the signal. By definition, the magnitude of α is considerably larger under condition 1 than under condition 0.

4. The condition detection algorithm

In this section the diagnostic algorithm is developed and discussed. In Section 4.1, the algorithm for distinguishing between conditions 0 and 1, which represents the main technical results of the paper, is developed. Attention is focused on conditions 0 and 1 since, as explained in Section 2, distinguishing conditions 2 and 3 is trivial. Section 4.2 discusses the implementation of the algorithm, in particular the computational expense. The overall diagnostic procedure for distinguishing all four conditions, as well as subsequent action to take in the event that each condition is detected, is outlined in Section 4.3. The diagnostic algorithm for distinguishing conditions 0 and 1 applies to either hex head bolts or Phillips head screws. The only implementation difference is in what frequency components are used to define the S_0 and S matrices.

4.1. Diagnosing conditions 0 and 1

The main idea behind the algorithm is to fit, in a least squares sense, the measured torque vector to the sinusoidal vectors contained in S_0 and S, where S_0 and S are defined by (1)

and (2). The extra sinusoids present in S are expected to be much more dominant under condition 1 than under condition 0. Thus, if the torque vector is approximated much more closely by the sinusoids in both S_0 and S than it is by only those in S_0, it will be concluded that condition 1 occurred.

Let P_0 denote the least squares projection operator onto the column space of S_0. Similarly, define $S_1 \equiv [S_0 \ S]$, and let P_1 denote the least squares projection operator onto the column space of S_1. Standard results from least squares theory give

$$P_0 = S_0 (S_0^T S_0)^{-1} S_0^T \tag{3}$$

$$P_1 = S_1 (S_1^T S_1)^{-1} S_1^T \tag{4}$$

Define $P_1^\perp$ to be the least squares projection operator onto the orthogonal complement of the column space of S_1, and define $P \equiv P_1 - P_0$. It follows from the definitions of $P_1^\perp$ and P that

$$P_1^\perp = I - P_1 \tag{5}$$

$$I = P_0 + P + P_1^\perp \tag{6}$$

where I is the identity matrix of appropriate dimension. The least squares approximation of the torque vector T by the sinusoids in S_0 and by those in S_1 are given, respectively, by

$$\hat{T}_0 \equiv P_0 T \tag{7}$$

$$\hat{T}_1 \equiv P_1 T \tag{8}$$

Defining the residual error vectors associated with these least squares approximations to be $E_0 \equiv T - \hat{T}_0$ and $E_1 \equiv T - \hat{T}_1$, it follows that

$$E_0 = [I - P_0]T = [P + P_1^\perp]T \tag{9}$$

$$E_1 = [I - P_1]T = P_1^\perp T \tag{10}$$

The first equalities in (9) and (10) follow from (7) and (8) and the second equalities from (5) and (6).

The residual sum of the squares for each of the least squares approximations then can be defined as $J_0 \equiv E_0^T E_0$ and $J_1 \equiv E_1^T E_1$. J_0 and J_1 are measures of how well the torque signal is approximated by linear combinations of the sinusoids used to construct S_0 and S_1, respectively. Intuitively, if $J_0 \gg J_1$, then including the extra sinusoids in S into the model provides a much better approximation of the torque signal. This, in turn, implies that condition 1 has occurred, since it was assumed that the sinusoids in S have significant energy under condition 1 and much smaller energy under condition 0. The remainder of this section is devoted to quantifying this intuitive argument.

Substituting (9) and (10) into the definitions of J_0 and J_1 gives

$$J_0 = T^T [P + P_1^\perp]^T [P + P_1^\perp] T = T^T P T + T^T P_1^\perp T \tag{11}$$

$$J_1 = T^T [P_1^\perp]^T P_1^\perp T = T^T P_1^\perp T \tag{12}$$

The second equalities in (11) and (12) follow by noting that $P_1^\perp$ and $P + P_1^\perp$ are both projection operators. Therefore, they are symmetric and idempotent (a square matrix A is defined to be idempotent if $A^2 = A$) and the results follow. That $P_1^\perp$ and $P + P_1^\perp$ are symmetric and idempotent also can be seen directly by substituting $I - P_1$ for $P_1^\perp$ and $I - P_0$ for $P + P_1^\perp$ and then substituting (3) and (4) for P_0 and P_1. From (11) and (12) it also follows that

$$J_0 - J_1 = T^T P T \tag{13}$$

The following statistic now can be defined as a measure of the improvement in the least squares fit gained by including the sinusoids in S:

$$F \equiv \frac{(J_0 - J_1)/2p}{J_1/(N - 2p_1 - 1)} \tag{14}$$

It follows from (11), (12), (13), and the Fisher-Cochran Theorem (Rao, 1973) that F follows a noncentral F-distribution with $2p$-numerator degrees of freedom and $(N - 2p_1 - 1)$-denominator degrees of freedom, denoted $F \sim F(2p, N - 2p_1 - 1, \lambda)$. In addition, the noncentrality parameter λ is given by

$$\lambda \equiv \frac{[S\alpha]^T [S\alpha]}{\sigma^2} - \frac{[S\alpha]^T P_0 [S\alpha]}{\sigma^2}$$

For an integer number of shaft revolutions, the sinusoids in S will be orthogonal to the sinusoids in S_0, and the second term in the expression for λ will vanish. For a noninteger number of shaft revolutions, although the second term may not be exactly 0, λ still will be dominated by the first term. Therefore, the noncentrality parameter λ has an interpretation as a signal-to-noise ratio. The term $[S\alpha]^T [S\alpha]$ is a measure of the energy in the torque signal due to the sinusoidal components with frequencies in Ω, and σ^2 is a measure of the noise power. Since the energy of the sinusoids with frequencies in Ω is assumed to be much larger under condition 1 than under condition 0, the noncentrality parameter will be much larger if condition 1 occurs and the distribution of F will shift significantly to the right.

This suggests using a noncentral F test to detect the presence of condition 1. Select a desired probability of false alarm η, and set the test threshold γ to be the $1 - \eta$ percentile of the $F(2p, N - 2p_1 - 1, \lambda)$ distribution. Here, λ is the noncentrality parameter under condition 0. When a torque measurement is obtained, F is calculated using (14) and compared to γ. If $F > \gamma$, conclude that condition 1 has occurred; and if $F \leq \gamma$, conclude condition 0 has occurred. Tables and approximations for the noncentral F distribution are available in Pearson and Hartley (1972).

Selection of γ requires that the value of λ under condition 0 be known. If none of the sinusoids in S is present under condition 0, then $\lambda = 0$ and a central F distribution can be used to select γ. If, however, the sinusoids in S have some energy under condition 0, $\lambda = 0$ cannot be assumed. Since the first moment of an $F(\nu_1, \nu_2, \lambda)$-distributed random variable

is $[\nu_2(\nu_1 + \lambda)]/[(\nu_2 - 2)\nu_1]$, an average value of F under condition 0 (denoted $\bar{F}$) can be calculated experimentally and λ can be estimated using

$$\lambda \cong \nu_1 \left[\left(\frac{\nu_2 - 2}{\nu_2} \right) \bar{F} - 1 \right]$$ (15)

The value of λ under condition 0 will depend somewhat on the characteristics of the screw (e.g., screw diameter), the hardware (e.g., internal gearing of the screwdriver), and the number of measurements N in the torque vector. Therefore, for a given experimental setup and class of screw, some training should be used to estimate λ under condition 0 and select an appropriate threshold.

Selecting the threshold so as to specify only the probability of false alarm has the advantage of not requiring knowledge of λ under condition 1. For the algorithm to diagnose the conditions effectively, it is enough to know that λ under condition 1 will be significantly larger than under condition 0. If one wished to select the threshold (for example) to minimize the Bayesian risk or if one wished to analyze the probability of correctly detecting condition 1, then knowledge of λ under condition 1 would be required as well. This is difficult to do in a generic sense, however, since λ under condition 1 will depend on additional factors, such as how worn the head of the screw is and how much thrust force is applied when attempting to unscrew it.

4.2. Implementation procedure and computational expense

This section outlines the suggested procedure for implementing the algorithm for distinguishing conditions 0 and 1 and discusses the computational expense. Implementation of the algorithm for distinguishing conditions 2 and 3 is straightforward, as discussed in Section 2. Computational expense is an important practical concern, since long delays in detecting the conditions could render the entire procedure inefficient. In addition, if condition 1 is not promptly detected, the tip of the screwdriver (or wrench) and the head of the screw (or bolt) quickly could be worn down.

At first glance it appears that implementation of the algorithm requires solving two least squares problems. However, the entire solution is not needed, since all that is required to calculate F is the sum of the squares of the residuals J_0 and J_1. These can be very efficiently calculated using QR factorization concepts. The idea is, after the S_1 matrix is constructed, to factor it into its QR form; that is, factor

$$S_1 = QR = \begin{bmatrix} q_1 & q_2 & \cdots & q_{2p_0+2p+1} \end{bmatrix} R$$ (16)

where Q is an $N \times (2p_0 + 2p + 1)$ matrix with orthonormal columns and R is a $(2p_0 + 2p + 1) \times (2p_0 + 2p + 1)$ upper triangular matrix. Here, q_i denotes the ith column of Q. See, for example, Golub and Van Loan (1990) for a detailed description of the QR factorization and computationally efficient algorithms for obtaining it.

Since the columns of $\mathbf{Q}$ are an orthonormal basis for the column space of $\mathbf{S}_1$, the least squares projection of T onto the column space of $\mathbf{S}_1$ is given by

$$\hat{T}_1 = \sum_{i=1}^{2p_0+2p+1} \left(q_i^T T\right) q_i$$

With the error vector E_1 defined as $T - \hat{T}_1$, it follows that

$$E_1 = T - \sum_{i=1}^{2p_0+2p+1} \left(q_i^T T\right) q_i$$

$$J_1 \equiv E_1^T E_1 = \left[T - \sum_{i=1}^{2p_0+2p+1} \left(q_i^T T\right) q_i\right]^T \left[T - \sum_{i=1}^{2p_0+2p+1} \left(q_i^T T\right) q_i\right]$$

$$= T^T T - 2T^T \sum_{i=1}^{2p_0+2p+1} \left(q_i^T T\right) q_i + \sum_{i=1}^{2p_0+2p+1} \left(q_i^T T\right) q_i^T \sum_{j=1}^{2p_0+2p+1} \left(q_j^T T\right) q_j$$

$$= T^T T - 2 \sum_{i=1}^{2p_0+2p+1} \left(q_i^T T\right)^2 + \sum_{i=1}^{2p_0+2p+1} \left(q_i^T T\right)^2$$

$$= T^T T - \sum_{i=1}^{2p_0+2p+1} \left(q_i^T T\right)^2 \tag{17}$$

where the third term in the second to last line results because the columns of $\mathbf{Q}$ are orthonormal. Since $\mathbf{S}_1 \equiv [\mathbf{S}_0\ \mathbf{S}]$, the Q matrix in the QR factorization of $\mathbf{S}_0$ is exactly the first $2p_0 + 1$ columns of $\mathbf{Q}$. Consequently, following the derivation of (17), it can also be shown that

$$J_0 = T^T T - \sum_{i=1}^{2p_0+1} \left(q_i^T T\right)^2 \tag{18}$$

To recognize the computational advantages of (17) and (18), first express T and the columns of $\mathbf{Q}$ in terms of their elements $T = [T_1\ T_2 \ \ldots\ T_N]^T$ and $q_i = [q_{1,i}\ q_{2,i}, \ldots, q_{N,i}]^T$. The columns of $\mathbf{Q}$ can be determined off-line since they depend only on $\mathbf{S}_1$. Writing the individual terms of (17) and (18) as

$$T^T T = \sum_{j=1}^{N} T_j^2 \tag{19}$$

$$q_i^T T = \sum_{j=1}^{N} q_{j,i} T_j \tag{20}$$

means that they can be updated recursively with only a few multiplications as each new sample of the torque signal is obtained (see the on-line portion of the algorithm that follows).

The entire procedure for distinguishing conditions 0 and 1 is divided into an off-line and on-line portion and summarized as follows.

Off-Line.

1. Based on the type of screw and the desired number of samples per shaft revolution, determine Ω_0 and Ω_1.
2. Determine the number (N) of samples that will constitute the torque signal or, equivalently, the number of shaft revolutions for which the torque signal will be measured. For all experiments conducted by the authors, two revolutions were sufficient. More or fewer may be suitable depending on the specific problem.
3. Select γ. This will require some training, via estimation of λ under condition 0 or under condition 1 or both.
4. Based on Ω_1 and N, construct S_1 according to (1) and (2).
5. Factor S_1 into its QR form, as in (16). The columns of Q will be used in the on-line portion.
6. Initialize the following dummy variables to be used in the on-line portion of the algorithm: $V_i = 0$ for $i = 1, 2, \ldots, 2p_0 + 2p + 1$.

On-Line. This assumes that the data acquisition is coordinated so that the torque signal is sampled uniformly with respect to shaft rotation.

1. At each sampling instant t ($t = 1, 2, \ldots, N$) take a new torque measurement T_t and update:

$$V_0 = V_0 + T_t^2 \quad \text{(for computing (19))}$$
$$V_i = V_i + q_{t,i}T_t, \quad \text{for } i = 1, 2, \ldots, 2p_0 + 2p + 1 \quad \text{(for computing (20))}$$

2. After N samples have been taken, calculate

$$J_0 = V_0 - \sum_{i=1}^{2p_0+1} V_i^2 \quad \text{(see (18))}$$

$$J_1 = J_0 - \sum_{i=2p_0+2}^{2p_0+2p+1} V_i^2 \quad \text{(see (17))}$$

$$F = \frac{(J_0 - J_1)/2p}{J_1/(N - 2p_1 - 1)}$$

3. Compare F to the threshold:
   If $F > \gamma$, conclude condition 1 occurred.
   If $F \leq \gamma$, conclude condition 0 occurred.

At each sampling instant, the on-line step 1 must be executed, requiring a total of only ($2p_0 + 2p + 2$) multiplications. After the Nth sample, on-line step 2 requires ($2p_0 + 2p + 3$)

multiplications. Consequently, the algorithm will cause almost no computational delay in diagnosing the conditions.

4.3. Algorithm flowchart

The implementation procedure of the previous section was for distinguishing between conditions 0 and 1. This section outlines the overall condition detection algorithm, including appropriate actions to take in the event that each condition is detected. Figure 4 shows a flowchart for the scheme. CW is used to denote clockwise and CCW denotes counterclockwise. At the *Begin* box it is assumed that a screw has been located with the vision system. The loops in the flowchart represent situations in which the screw does not come out on the first attempt (condition 1, 2, or 3 occurred) and, after making suitable adjustments, another attempt is made. The box to the left of loop 3 and the two boxes to the right of loops 1 and 2 represent situations in which the screw will not come out at all. For example, consider loop 1, which the algorithm enters if condition 1 is detected. Since this condition represents the screwdriver slipping on the head of the screw it may be desirable to increase the
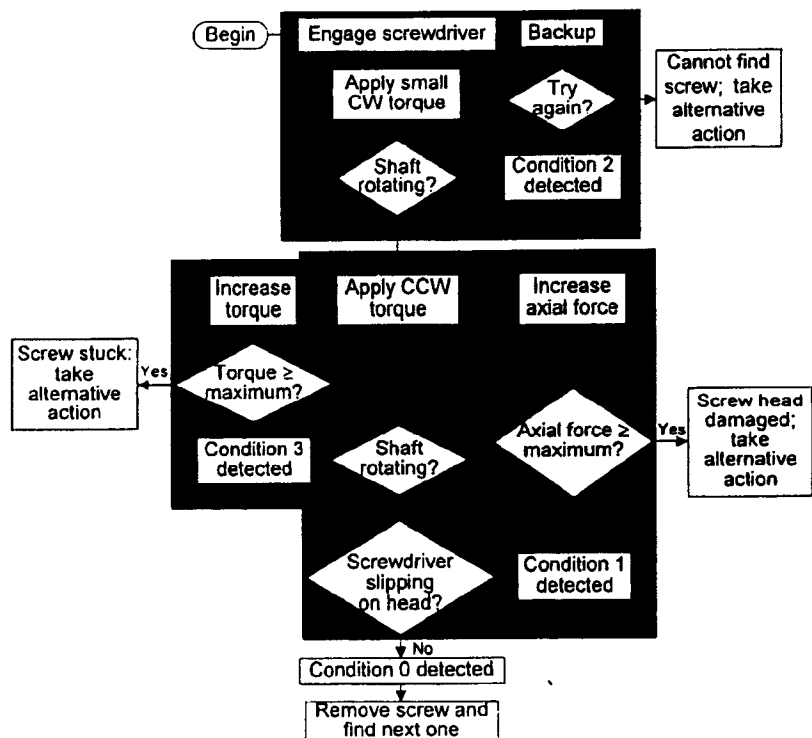

Figure 4. Flowchart for the condition detection algorithm.

axial force on the screwdriver and try again. If the axial force already is greater than some prespecified maximum, then one can conclude that the screw head is too worn to engage properly with the screwdriver. Some alternative action (for example, milling or drilling the screw head) must be taken. Likewise, if condition 3 is detected (i.e., the screw is too tight to be loosened using the current torque) the algorithm enters loop 3. It then may be desirable to increase the torque and try again. If the torque already is greater than some prespecified maximum, one can conclude that the screw is too tight to be removed and, again, mill or drill the screw head. Similarly, if condition 2 is detected repeatedly, one can conclude that the screw cannot be properly located with the vision system.

The entire flowchart applies to Phillips head screws and hex head bolts. As mentioned in Section 2, the condition 1 category is not applicable to slot head screws. Consequently, only the portion of the flowchart distinguishing conditions 2 and 3 should be implemented when attempting to remove slot head screws.

Cutting the screw out, if it cannot be turned out, is considered acceptable in this research. However, it is considered a less desirable alternative than removing it nondestructively, as discussed in Section 2. Consequently, cutting the screw is considered only as a last resort when the screw cannot be removed nondestructively.

5. Experimental results

The experimental setup is shown in figure 1. As explained in Section 2, detection of conditions 2 and 3 is quite easy to accomplish. Therefore, the results presented in this section are for detecting condition 0 (screw coming out) or condition 1 (screwdriver slipping on screw head) for a Phillips head screw. Experimental results for hex head bolts were nearly identical, except that the fundamental frequency component in the torque signal was 6ω instead of 4ω.

The parameters $\Omega_0 = \{0, \omega, 2\omega, 3\omega\}$ and $\Omega_1 = \{0, \omega, 2\omega, 3\omega, 4\omega, 8\omega, 12\omega, 16\omega, 20\omega\}$ were chosen, resulting in $p_0 = 3$, $p = 5$, and $p_1 = 8$. The sampled torque signal T consists of $N = 572$ torque measurements over two shaft revolutions. Using (15), λ under condition 0 was estimated experimentally as $\lambda \cong 95.3$. Based on this estimate, a threshold $\gamma = 16.84$ was selected to provide a probability of false alarm 0.5%.

The data under condition 0 is shown in figure 5(a) and under condition 1 in figure 5(b). In both figures, T is the original torque signal, $\hat{T}_0$ represents the least squares fit of T using the sinusoids in S_0, and $\hat{T}_1$ represents the least squares fit using the sinusoids in S_1 (i.e., the sinusoids in S_0 plus the extra sinusoids in S). Note the scaling difference of the torque axes in the two figures. Under condition 0, including in the model the extra sinusoids in S does not greatly improve the least squares fit so that $\hat{T}_1$ approximates T only slightly better than $\hat{T}_0$. Consequently, there is only a slight reduction in the residual sum of the squares, and $F = 10.22$ lies below the threshold. Under condition 1, including the extra sinusoids significantly improves the least squares fit, and the resulting $F = 307.3$ lies far above the threshold. Thus, condition 1 was easily detected. Table 1 shows experimental results for four tests under condition 0 and four under condition 1. Since the values of F are much larger under condition 1 than under condition 0, the two conditions can be distinguished readily.

Table 1. Experimentally calculated values of F.

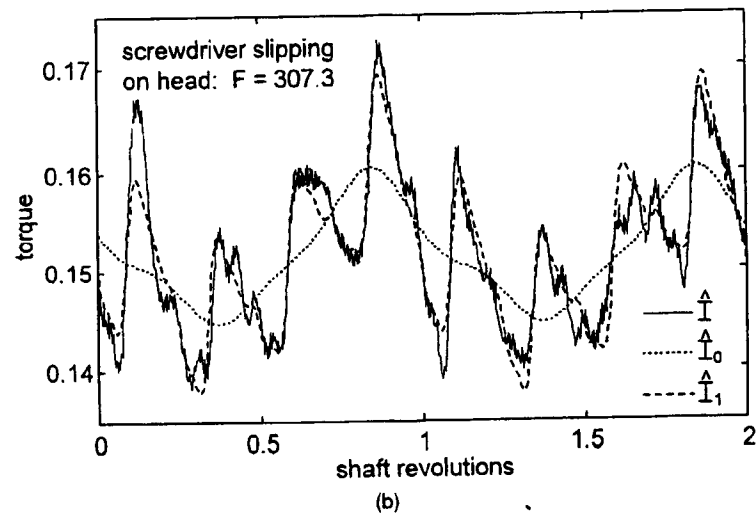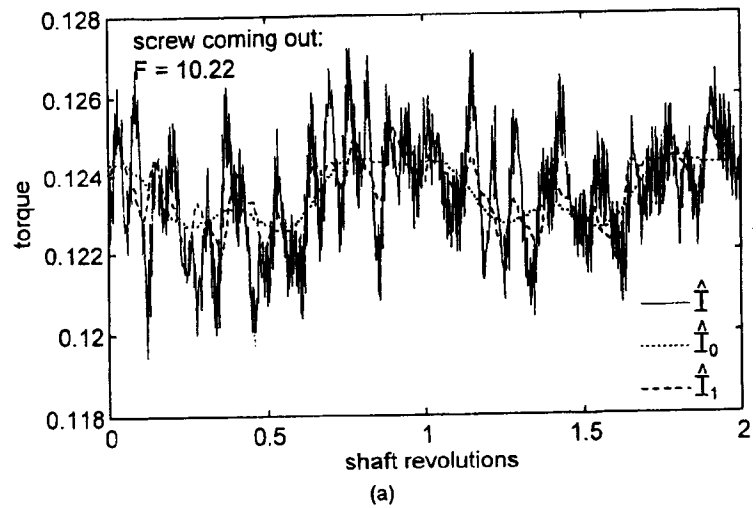|	Experimental F value			
Condition 0	8.65	10.22	13.05	2.31
Condition 1	366.4	457.1	307.3	129.2

Figure 5. Actual and least squares fitted torque signals when: (a) condition 0 occurred and (b) condition 1 occurred.

6. Conclusions

Due to growing interest in environmentally friendly manufacturing and recycling, disassembly is a major area of research. Many technical challenges are involved in successfully designing and implementing a disassembly operation. A critical issue is how to determine exactly what is happening when one attempts to unscrew and remove a screw; that is, the screw coming out and, if not, why not? This paper presents an algorithm for diagnosing the unscrewing process and deciding what to do if the screw is not coming out.

One conclusion of this research is that, by measuring only the unscrewing torque and shaft rotation, one can accurately diagnose which condition arises during unscrewing. The majority of the diagnostics reduces to deciding between one of two conditions: Is the screw coming out or is the screwdriver slipping on the head of the screw? For determining this, a straightforward, computationally efficient, least-squares-based algorithm has been developed. The experimental results demonstrate that the algorithm is highly successful in detecting which of these conditions has occurred.

References

Boothroyd, G. and Alting, L., "Design for Assembly and Disassembly," *CIRP Annals*, Vol. 41, No. 2, pp. 1–12 (1992).

Dario, P., Rucci, M., Guadagnini, C., and Laschi, C., "An Investigation on a Robot System for Disassembly Automation," *Proceedings of the 1994 IEEE International Conference on Robotics and Automation*, pp. 3515–3521 (1994).

de Ron, A. and Penev, K., "Disassembly and Recycling of Electronic Consumer Products: An Overview," *Technovation*, Vol. 15, No. 6, pp. 363–374 (1995).

Dutta, D. and Woo, T.C., "Algorithm for Multiple Disassembly and Parallel Assemblies," *ASME Journal of Engineering for Industry*, Vol. 117, No. 1, pp. 102–109 (1995).

Feldmann, K. and Scheller, H., "Disassembly of Electronic Products," *Proceedings of the 1994 IEEE International Symposium on Electronics and the Environment*, pp. 81–86 (1994).

Golub, G.H. and Van Loan, C.F., *Matrix Computations*, 2nd ed., Johns Hopkins University Press, Baltimore (1990).

Hentschel, C., Seliger, G., and Zussman, E., "Recycling Process Planning for Discarded Complex Products: A Predictive and Reactive Approach," *Proceedings of the Second International Seminar on Life Cycle Engineering*, Erlangen, Germany, pp. 195–209 (October 1994).

Hentschel, C., Seliger, G., and Zussman, E., "Grouping of Used Products for Cellular Recycling Systems," *CIRP Annals—Manufacturing Technology*, Vol. 44, No. 1, pp. 11–14 (1995).

Jorgensen, T., Andersen, A., and Christensen, S., "Shape Recognition System for Automatic Disassembly of TV Sets," *Proceedings of the 1996 IEEE International Conference on Image Processing*, pp. 653–656 (1996).

Juvinal, R.C., *Fundamentals of Machine Component Design*, John Wiley and Sons, New York (1983).

Kopacek, P. and Kronreif, G., "Semi-Automated Robotized Disassembling of Personal Computers," *Proceedings of the IEEE Symposium on Emerging Technologies and Factory Automation*, pp. 567–572 (1996).

Langerak, E., "To Shred or Disassemble? Recycling of Plastics in Mass Consumer Goods," *Proceedings of the 1997 IEEE International Symposium on Electronics and the Environment*, pp. 63–68 (1997).

Navin-Chandra, D., "Design for Environmentability," *Third International Conference on Design Theory and Methodology*, ASME Design Engineering Division, Vol. DE-31, pp. 119–125 (September 1991).

Pearson, E. and Hartley, H., eds., *Biometrika Tables for Statisticians*, Vol. 2, Cambridge University Press, London, England (1972).

Rao, C.R., *Linear Statistical Inference and its Applications*, 2nd ed., John Wiley and Sons, New York (1973).

Ray, L., "Robot Disassembles Explosive Devices," *Industrial Robot*, Vol. 23, No. 3, pp. 20–24 (1996).

Seliger, G., Hentschel, C., and Kriwet, A., "Recycling and Disassembly—Legal Burden or Strategic Opportunity?" *Proceedings of the Second Workshop of Assembly Automation and Future Outlook of Production Systems*, Tokyo, pp. 89–95 (November 1993).

Seliger, G. and Hentschel, C., "Disassembly Process Planning to Support the Recyclability of Used Technical Products," *Proceedings of the Vision EUREKA Conference: Industrial Opportunities in Waste Management*, Lillehammer, Norway, pp. 194–201 (June 1994).

Weigl, A., "Requirements for Robot Assisted Disassembly of Not Appropriately Designed Electronic Products: Lessons from First Studies," *Proceedings of the 1994 IEEE International Symposium on Electronics and the Environment*, pp. 337–342 (1994).

Zussman, E., Kriwet, A., and Seliger, G., "Disassembly-Oriented Assessment Methodology to Support Design for Recycling," *CIRP Annals*, Vol. 43, No. 1, pp. 9–14 (1994).